IEEE Access
Multidisciplinary | Rapid Review | Open Access Journal

Received November 28, 2017, accepted February 7, 2018, date of publication February 12, 2018, date of current version March 16, 2018.

Digital Object Identifier 10.1109/ACCESS.2018.2805306

A Nonlinear ARMA-GARCH Model With Johnson S_u Innovations and Its Application to Sea Clutter Modeling

YUNJIAN ZHANG, HUI LIU, YANAN HUANG, AND ZHENMIAO DENG, (Member, IEEE)
School of Information Science and Engineering, Xiamen University, Xiamen 361005, China

Corresponding author: Yunjian Zhang (yunjzhang@xmu.edu.cn)

This work was supported in part by the National Natural Science Foundation of China under Grant 61471012 and in part by the Open-End Fund of BITTT Key Laboratory of Space Object Measurement.

ABSTRACT In this paper, a novel time series heteroskedastic model is proposed for sea clutter modeling application. In the light of characteristics of the practical clutter at low grazing angle, the original generalized autoregressive conditional heteroskedasticity process, which has been widely used in various fields of economics, is extended from three aspects. First, the autoregressive moving-average terms are introduced for modeling the temporal correlation of both clutter returns and innovations. Second, the exponential of the conditional variance is generalized from one to arbitrary positive value, to capture the nonlinearity existing in the practical clutter. Third, the traditional Gaussian innovation is replaced by the Johnson S_u random variable, which is a monotonic transformation of the Gaussian random variable and is capable of modeling the skewness and kurtosis. By systematically analyzing a large number of practical sea clutter data sets, we show that the proposed time series model fits the data better than some commonly used statistic-based distributions, such as the Weibull and compound Gaussian distributions.

INDEX TERMS Radar, sea clutter modeling, ARMA, GARCH, Johnson S_u distribution.

I. INTRODUCTION

The accurate modeling of sea clutter is of great importance for remote sensing and radar signal processing. Under different environment conditions, viewing geometries, and radar operating parameters, the characteristics of sea clutter may vary extremely widely [1]–[4]. In general, sea clutter is more spiky at lower grazing angles and higher spatial resolution, and horizontally polarized returns are more spiky than those for vertical polarization [5]. As a result, the probability distribution of the practical clutter is often leptokurtic, i.e., heavy-tailed. Further, under the influence of a series of external conditions, e.g., wind and gravity, sometimes the clutter shows skewness and nonlinearity. It is also worth mentioning that a common and adaptive clutter model is supposed to be capable of accurate modeling of temporal and spatial correlation features.

Over the past several decades, a number of non-Gaussian distributions has been proposed, including Weibull [6]–[8], K [9], log-normal [10], compound-Gaussian [11]–[13], Tsallis [14], etc. However, the fitting of these statistics-based distributions to practical clutter data is lack of flexibility at times. For instance, when the radar polarization mode or grazing angle changes, the original clutter model may no longer be applicable, or lead to a decrease in fitting performance. In [15], Pascual *et al.* use economic generalized autoregressive conditional heteroskedasticity (GARCH) process [16] for sea clutter modeling. Let η_t denote a real-valued stochastic process, the GARCH(m,n) process is then given by

$$\eta_t = \sqrt{h_t}\varepsilon_t \tag{1}$$

$$h_t = \alpha_0 + \sum_{i=1}^{m} \alpha_i \eta_{t-i}^2 + \sum_{j=1}^{n} \beta_j h_{t-j} \tag{2}$$

where h_t denotes the time-varying variance, ε_t is the so-called innovation, which satisfies certain distribution. It is necessary to add some restrictions on the model coefficients $\{\alpha_i\}_{i=0}^{m}$, and $\{\beta_j\}_{j=1}^{n}$ to make sure that h_t is finite and stationary, see [16] for more details. It is seen from (2) that the model uses the process history to improve its current feature. Moreover, the GARCH process can measure the implied volatility of a time series, and its PDF is heavy-tailed. These characteristics make it suitable for sea clutter modeling application. It is worth mentioning that in recent years, the GARCH process

also has been used in synthetic aperture radar (SAR) imaging and sonar fields [17], [18]. The analysis results of practical sea clutter data [15] show that this more flexible time series modeling method adequately represents the statistics of the data, and outperforms the Gaussian and Weibull distributions. In [19], Pascual *et al.* extend the one-dimensional GARCH process to the 2D case, the advantage of which is that it can simultaneously consider the influence of both adjacent fast and slow time dimensional information to current clutter returns. Also, the introduction of autoregressive (AR) terms in the conditional mean expression is able to model the correlation of slow time dimension to a certain degree.

On the other hand, however, the original GARCH process also has some limitations in sea clutter modeling application. First, the structure of conditional variance is relatively simple, which is the linear combination of square of past returns and past conditional variances. In practical situation, most environment factors are unpredictable, and the conditional variance often shows nonlinearity and asymmetry [20], [21]. Second, for high resolution maritime radars with pulse repetition frequency ranges from several hundred hertz to several thousand hertz, the correlation (especially temporal correlation) of the clutter return is significant, which cannot be accurately modeled by GARCH or AR-GARCH process [22]. Third, the innovation of GARCH process is commonly assumed to satisfy Gaussian distribution, Student-t distribution [23], generalized-t distribution [24], or the generalized error distribution (GED) [25]. It is clear that all these distributions are symmetric, which are incapable of modeling the skewness existing in practical clutter data.

Therefore, combining with the above mentioned issues, we propose a novel nonlinear autoregressive moving-average GARCH (ARMA-NGARCH) model with Johnson S_u (JSU) innovations in this paper. The ARMA terms are used for modeling the temporal correlations of both clutter returns and innovations. The nonlinear exponential of conditional variance generalized the traditional linear expression to adapt to more general situations. The JSU random variable (RV) [26] is skewed and leptokurtic. The skewness and the kurtosis of the JSU distribution can be controlled by the shape parameters. It is noted that there are also some other skewed and leptokurtic distributions, such as the skewed-t [27] and skewed GED [28] distributions. The advantage of the JSU distribution is its simplicity and ease of use, since it only requires a monotonic transformation of the normal distribution. Through comprehensive analyses of practical sea clutter data sets, it is proved that the proposed model achieves excellent fitting performance in aspects of amplitude and temporal correlation, comparing with some commonly used statistic-based distributions, such as the Weibull and compound Gaussian (CG) distributions.

The rest of the paper is organized as follows. Section II briefly introduces the proposed ARMA-NGARCH-JSU model. In Section III, the parameter estimation algorithm is presented. The statistical analyses of practical sea clutter databases are given in Section IV. In Section V, some numerical simulations are conducted to validate the advantages of the proposed model. Finally, Section IV summarizes this work and draws the conclusion.

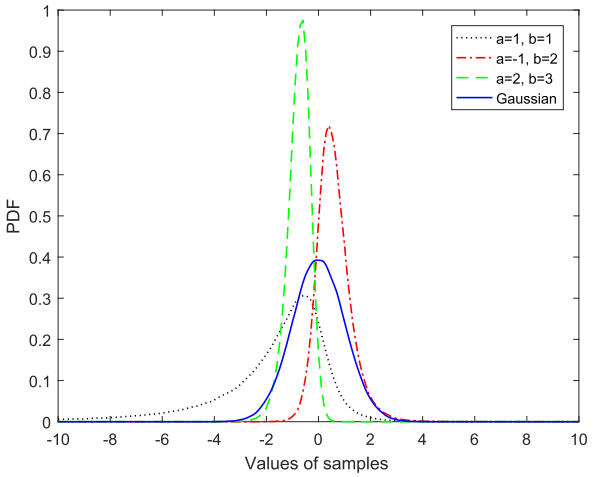

FIGURE 1. PDFs of standard normal distribution, and of the JSU distributions corresponding to various settings of the shape coefficients a and b.

II. NOVEL CLUTTER MODEL

It is assumed that the clutter measurements are described by the following ARMA-NGARCH process y_t

$$y_t = \sum_{i=1}^{p} \varphi_i y_{t-i} + \sum_{j=1}^{q} \phi_j \eta_{t-j} + \eta_t \tag{3}$$

$$\eta_t = \sqrt{h_t}\varepsilon_t \tag{4}$$

$$h_t^{\delta} = \alpha_0 + \sum_{i=1}^{m} \alpha_i h_{t-i}^{\delta} + \sum_{j=1}^{n} \beta_j \left(\eta_{t-j}^2\right)^{\delta} \tag{5}$$

where positive integers p, q, m, and n are model orders; φ_i and ϕ_j are AR and MA coefficients of the conditional mean, respectively. $\alpha_0 > 0$, $\alpha_i \geq 0$, and $\beta_i \geq 0$ are coefficients of conditional variance h_t, while the restrictions on them guarantee the positivity of h_t. δ is the nonlinear coefficient of the conditional variance h_t. The innovation term ε_t is specified as the JSU RV with mean zero and unit variance. More specifically, assuming z is a standard normal RV, ζ satisfies the JSU distribution if

$$\zeta = \sinh\left(\frac{z-a}{b}\right) \tag{6}$$

where $\sinh(x) = (e^x - e^{-x})/2$ is the hyperbolic function, a and b are shape parameters controlling the skewness and kurtosis with $-\infty < a < \infty$ and $b > 0$. That is, a positive (negative) value of a induces a negative (positive) skewness, while smaller (higher) values of b are associated with larger (smaller) kurtosis values. Fig. 1 shows some PDFs of the JSU distributions corresponding to different shape coefficients a and b.

The inverse of the transform (6) is given by

$$z = a + b\sinh^{-1}(\zeta) \tag{7}$$

In [29], it is shown that the expected value and variance of ζ can be expressed as the following closed form

$$M_\zeta = -\sqrt{\omega}\sinh(\Omega) \tag{8}$$

$$V_\zeta = \frac{1}{2}(\omega - 1)[\omega\cosh(2\Omega) + 1] \tag{9}$$

where $\cosh(x) = (e^x + e^{-x})/2$, $\omega = \exp(1/b^2)$, and $\Omega = a/b$. Therefore, we can define ε_t as a standardized JSU RV, which can be written as [30]

$$\varepsilon_t = \frac{\zeta_t - M_\zeta}{\sqrt{V_\zeta}} \tag{10}$$

Comparing with the direct form of (6), the definition of (10) makes η_t a zero-mean RV with conditional variance h_t, and therefore, makes the interpretation of the GARCH variances more concise [30].

III. PARAMETER ESTIMATION

Under many circumstances, the maximum likelihood estimators have a number of desirable properties. However, it is generally infeasible to pursue a full exact likelihood approach, since the joint distribution of a sequence of observations $(y_1, \ldots, y_N)$ from a nonlinear ARMA-GARCH process driven by JSU innovations is very difficult to derive. Instead, conditional maximum likelihood estimation is quite straightforward to implement. The resulting conditional maximum likelihood estimates, often called quasi-maximum likelihood estimates (QMLEs), are always consistent and asymptotically normally distributed under some mild conditions [31]. For the proposed ARMA-NGARCH-JSU process, the conditional log-likelihood function (LLF) for the residuals η_t can be written as

$$L = -\frac{1}{2}\sum_{t=1}^{N}\ln h_t + \sum_{t=1}^{N}\ln f_{\varepsilon_t} \tag{11}$$

where f_{ε_t} is the probability density function (PDF) of ε_t. Since ε_t is a transformation of the standard normal RV, f_{ε_t} can be obtained by taking advantage of the following relationship

$$f_{\varepsilon_t} = f_{z_t} \times \left|\frac{\partial z_t}{\partial \varepsilon_t}\right| \tag{12}$$

where f_{z_t} is the PDF of a standard normal RV. According to (7) and (10), we can write $z_t = a + b\sinh^{-1}\left(M_\zeta + \varepsilon_t\sqrt{V_\zeta}\right)$. Ignoring the constant term, (11) can then be written as

$$L = -\frac{1}{2}\sum_{t=1}^{N}\ln h_t - \frac{1}{2}\sum_{t=1}^{N}\left[a + b\sinh^{-1}\left(M_\zeta + \varepsilon_t\sqrt{V_\zeta}\right)\right]^2 + \frac{N}{2}\ln V_\zeta + N\ln b - \frac{1}{2}\sum_{t=1}^{N}\ln\left[\left(M_\zeta + \varepsilon_t\sqrt{V_\zeta}\right)^2 + 1\right] \tag{13}$$

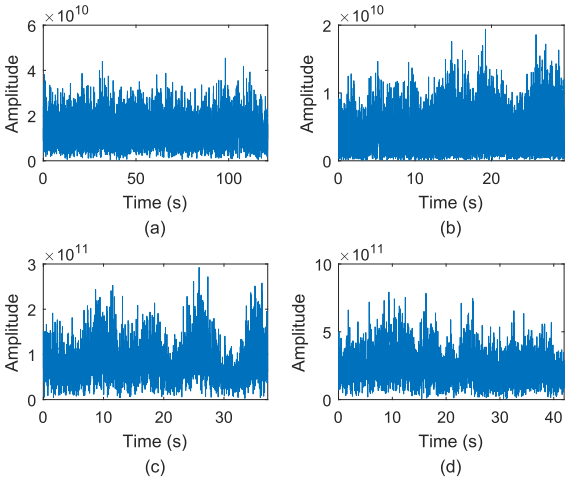

FIGURE 2. Time histories of clutter amplitude in a range cell for randomly selected four groups of data. (a) Range cell 85 of data 005. (b) Range cell 88 of data 012. (c) Range cell 1 of data 021. (d) Range cell 1 of data 026.

where h_t is defined by (5). Then, the QMLEs are obtained by maximizing (13), which can be completed through some numerical methods (e.g., Newton and quasi-Newton methods). In this paper, the popular Broyden-Fletcher-Goldfarb-Shanno (BFGS) quasi-Newton method is adopted due to its convergence and superlinear convergence rate, see [32] for a detailed introduction.

IV. STATISTICAL ANALYSES OF PRACTICAL SEA CLUTTER DATABASES

To evaluate the fitting accuracy of the proposed ARMA-NGARCH-JSU model for practical data, a clutter database is utilized in this paper. That is, the Council for Scientific and Industrial Research (CSIR) database, which contains a significant amount of suitable data recorded under different environment conditions, the geometry of the radar deployment site, and the radar system operating parameters [33].

In 2007, the X-band monopulse radar was deployed on Signal Hill, 33°55′15.62″ S, 18°23′53.76″ E, 308 m above mean sea level. The shortest distance to the coast line was 1250 m at a bering of 288° N. The site provided 140° azimuth coverage from 250° N to 20° N, of which a large sector spanned open sea whilst the remainder looked towards the West Coast coastline from the direction of the open sea [34]. Specifically, we obtain 13 groups of clutter measurements recorded in November 4th. The radar transmitting frequency is 8.8 GHz and the range resolution is 15 m. Other radar setups and environment conditions are summarized in Table 1, including height and direction of the wave, elevation angle and azimuth angle of the antenna, etc.

Fig. 2 shows time histories of the clutter amplitude in different range cells from randomly selected four groups of data. Clearly, there is a significant difference between different data sets. Since both transmitted and received signals have vertical polarization, the sea clutter is not very spiky. However, the presence of spikes is evident. It is known that the in-

TABLE 1. Summary of radar setups and environment conditions of the CSIR database recorded in November 4th, 2007.

Data	PRF (kHz)	Duration (s)	Range (m)	Grazing Angle (°)	Wave (Significant wave height)	Antenna Azm. (°)	Antenna Elv. (°)
005	2	121.095	1499	3.76 to 5.56	2.84 m, 264 N (4.7 m)	352.9 to 354.4 N	-5.131 to -4.916
010	2	32.0775	1499	5.56 to 10.6	2.84 m, 264 N (4.7 m)	311.2 to 313.7 N	-8.399 to -8.174
011	2	34.2225	1499	4.67 to 7.78	2.62 m, 261.7 N (4.5 m)	293.2 to 293.3 N	-5.845 to -5.62
012	1	29.502	1499	4.49 to 7.29	2.62 m, 261.7 N (4.5 m)	293.4 to 293.6 N	-5.433 to -5.246
014	2	60.2175	1499	3.53 to 5.08	2.62 m, 261.7 N (4.5 m)	289.8 to 292.4 N	-4.4 to -4.175
016	2	55.2825	1499	2.99 to 4.02	2.62 m, 261.7 N (4.5 m)	287.5 to 288 N	-3.499 to -3.384
017	1	49.17	1499	2.84 to 3.76	2.62 m, 261.7 N (4.5 m)	289 to 289.6 N	-3.252 to -3.159
018	1	52.832	1499	2.71 to 3.53	2.62 m, 261.7 N (4.5 m)	289.7 to 290.1 N	-3.148 to -3.126
020	2	68.82	1499	2.53 to 3.24	2.62 m, 261.7 N (4.5 m)	288.3 to 288.5 N	-2.966 to -2.884
021	2	32.2775	1499	2.84 to 3.76	2.62 m, 261.7 N (4.5 m)	288.3 to 288.9 N	-3.323 to -3.186
022	1	36.058	1499	2.71 to 3.53	2.64 m, 262.7 N (4.5 m)	289.8 to 290.3 N	-3.219 to -3.115
025	2	32.3375	599.6	2.53 to 2.77	2.64 m, 262.7 N (4.5 m)	286.3 to 286.5 N	-2.714 to -2.637
026	2	41.943	539.6	2.39 to 2.58	2.64 m, 262.7 N (4.5 m)	284.4 to 285.5 N	-2.587 to -2.521

TABLE 2. Statistics for data 018.

Range Cell	Component	Jarque-Bera	$Q^2(1)$	$Q^2(5)$	$Q^2(10)$	$Q^2(20)$	$Q^2(30)$
1	I	349.45	43974.05	90807.85	92773.01	92871.95	92884.81
		(0.00)	(0.00)	(0.00)	(0.00)	(0.00)	(0.00)
1	Q	143.43	43642.80	87165.57	88147.74	88159.35	88175.19
		(0.00)	(0.00)	(0.00)	(0.00)	(0.00)	(0.00)
10	I	493.85	42129.12	79404.63	80678.96	80783.12	80808.79
		(0.00)	(0.00)	(0.00)	(0.00)	(0.00)	(0.00)
10	Q	470.04	42140.31	79532.38	80886.94	80916.81	80940.20
		(0.00)	(0.00)	(0.00)	(0.00)	(0.00)	(0.00)
30	I	203.79	42569.70	83603.05	84285.05	84313.18	84320.64
		(0.00)	(0.00)	(0.00)	(0.00)	(0.00)	(0.00)
30	Q	99.70	42780.52	85841.52	87027.40	87284.25	87354.54
		(0.00)	(0.00)	(0.00)	(0.00)	(0.00)	(0.00)
80	I	194.44	42471.03	80040.76	81180.63	81589.99	81639.11
		(0.00)	(0.00)	(0.00)	(0.00)	(0.00)	(0.00)
80	Q	118.77	42407.60	79457.53	80349.21	80440.43	80508.99
		(0.00)	(0.00)	(0.00)	(0.00)	(0.00)	(0.00)
100	I	31.62	43088.70	80064.03	80241.17	80287.53	80318.82
		(0.00)	(0.00)	(0.00)	(0.00)	(0.00)	(0.00)
100	Q	28.98	43029.90	79425.32	79597.26	79680.41	79691.88
		(0.00)	(0.00)	(0.00)	(0.00)	(0.00)	(0.00)

[1] The p-values are reported in parentheses.

phase (I) and quadrature (Q) components of high resolution sea clutter data at low grazing angles have a non-Gaussian PDF, and hence, the amplitude of received clutter measurements is not Rayleigh distributed. For quantitative analysis of deviation of the CSIR data from Gaussian, we analyze the skewness and kurtosis of empirical PDFs of I and Q components. Skewness characterizes the degree of asymmetry of a distribution around its mean value, and kurtosis measures the peakedness or flatness of a distribution. The skewness and kurtosis of a RV Z are respectively defined as follows [35]

$$\left(\gamma_3^Z\right)_{I,Q} = \frac{E\left\{\left[Z_{I,Q} - E\left(Z_{I,Q}\right)\right]^3\right\}}{E\left\{\left[Z_{I,Q} - E\left(Z_{I,Q}\right)\right]^2\right\}^{3/2}} \tag{14}$$

$$\left(\gamma_4^Z\right)_{I,Q} = \frac{E\left\{\left[Z_{I,Q} - E\left(Z_{I,Q}\right)\right]^4\right\}}{E\left\{\left[Z_{I,Q} - E\left(Z_{I,Q}\right)\right]^2\right\}^2} \tag{15}$$

For the normal distribution, the skewness is 0 and the kurtosis is 3. The values of skewness and kurtosis of data 011, for example, is shown in Fig. 3. We use the first 35 range cells which contain clutter only. It is seen that in most cases, the asymmetry is significant and the peakedness is larger than 3.

Next, we analyze the temporal and spatial correlation properties of the CSIR data. In Fig. 4, the temporal autocorrelation functions (ACFs) of I component of data 018 from lag 0 to 50 are plotted. Four range cells are randomly chosen, i.e., range cell 4, 20, 60, and 100. The blue lines show 95% confidence interval for the estimated sample ACF if the clutter measurements are independently and identically distributed (IID). Taking Fig. 4(a) as an example, the first five lag autocorrelations are 0.9304, 0.8058, 0.6587, 0.5235, and 0.4177, respectively, which are significant positive. About 43% of the autocorrelations stay outside the confidence interval, which proves the strong temporal correlations in practical clutter measurements. Moreover, the autocorrelation characteristics for different range cells have considerable discrepancy, which demonstrates that the CSIR data is inhomogeneous.

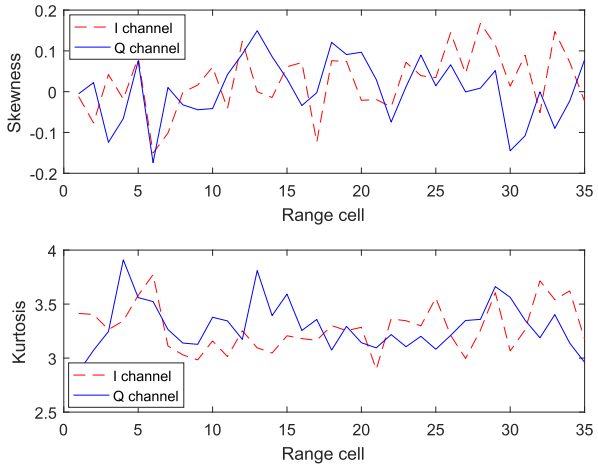

FIGURE 3. Skewness and kurtosis of I and Q component PDFs for the first 35 range cells of data 011.

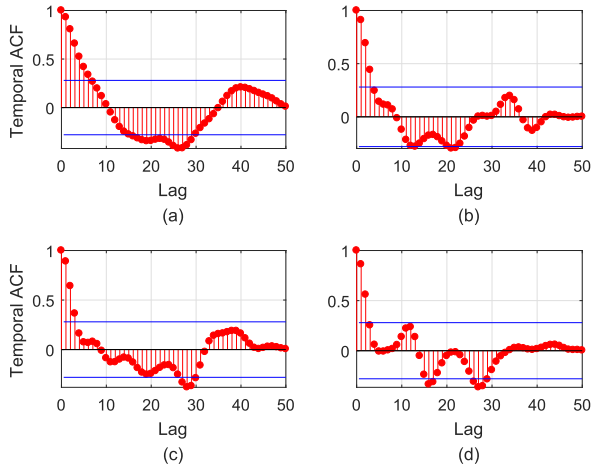

FIGURE 4. Temporal ACF of I component of data 018. (a) Range cell 4. (b) Range cell 20. (c) Range cell 60. (d) Range cell 100.

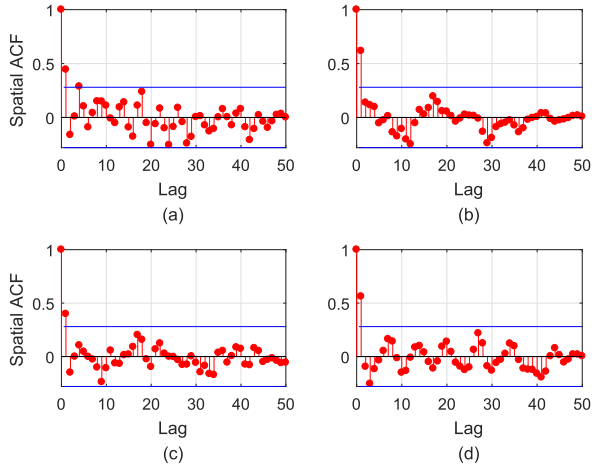

FIGURE 5. Spatial ACF of I component of data 018. (a) The 10th pulse. (b) The 2000th pulse. (c) The 3500th pulse. (d) The 9000th pulse.

Fig. 5 shows the spatial correlation properties of I component of data 018. The four subplots correspond to four randomly selected pulses. Due to the fact that the radar range resolution is 15 m, the spatial correlation is relatively weak, comparing with the temporal correlation. This is also the reason that we restrict the proposed model to the 1D case. Note that we ignore the analysis of Q components, since the autocorrelation characteristics of which is similar to that of I components.

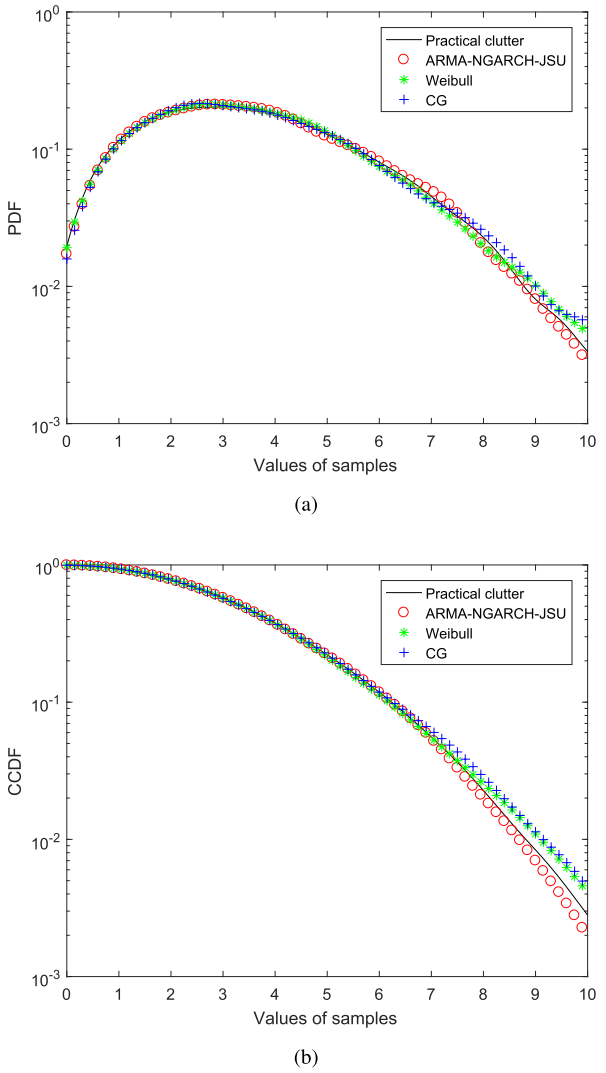

FIGURE 6. Fitted PDFs (a) and CCDFs (b) for the 1st range cell of data 005.

Taking data 018 as an example, the more comprehensive test results for different range cells are reported in Table 2. In statistics, the Jarque-Bera test is a goodness-of-fit test of whether sample data have the skewness and kurtosis matching a normal distribution, see [36] for more details. The test results show that the null hypotheses of normality are strongly rejected for both I and Q components of all data from five range cells. Also, the Ljung-Box Q-test [37] on the squared series, $Q^2(1)$ to $Q^2(30)$, reported in the last five columns of Table 2 indicate significant presence of volatility clustering or time dependent heteroscedasticity in clutter returns at lag length of 1 to 30.

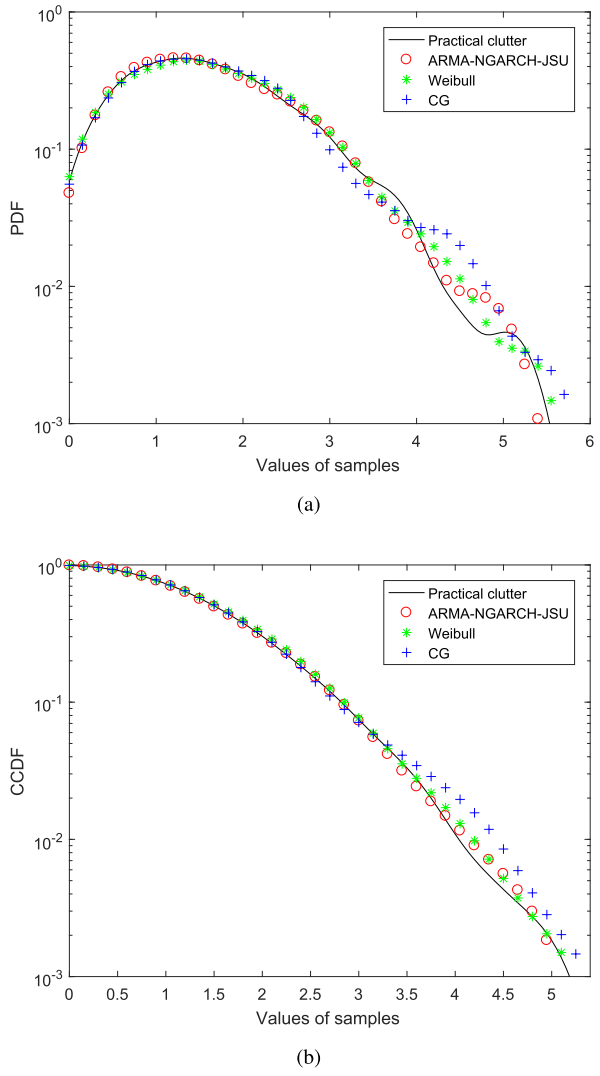

FIGURE 7. Fitted PDFs (a) and CCDFs (b) for the 1st range cell of data 011.

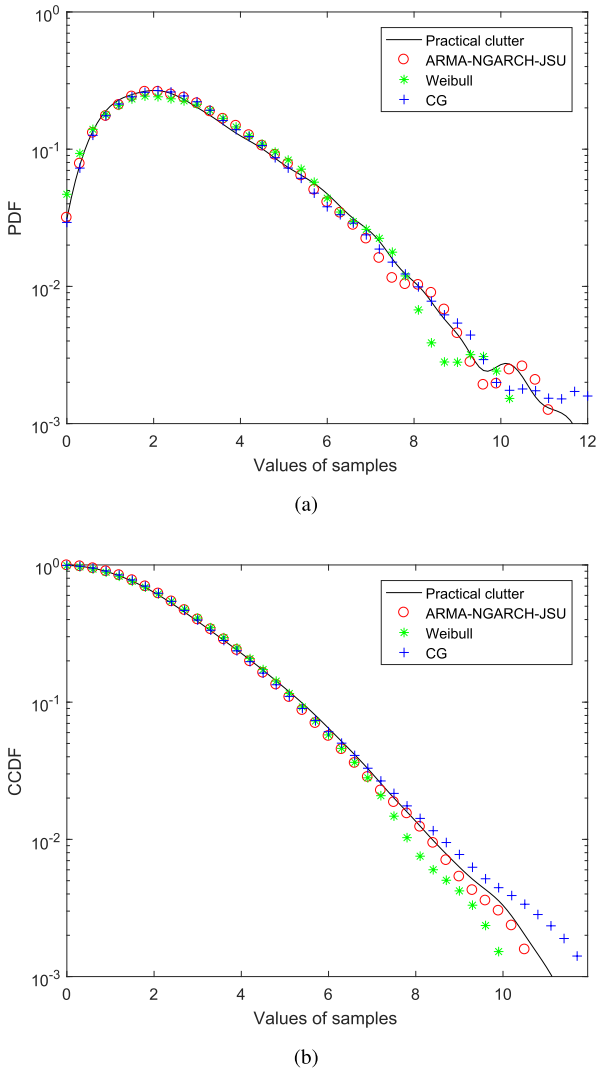

FIGURE 8. Fitted PDFs (a) and CCDFs (b) for the 20th range cell of data 020.

V. SIMULATION RESULTS

In this section, we investigate the capabilities of the proposed ARMA-NGARCH-JSU model to fit the practical complementary cumulative distribution function (CCDF) for various data sets. For comparative purpose, we chose Weibull distribution and CG distribution (with inverse Gamma texture) as the benchmarks, which both have been widely used for sea clutter modeling, see, e.g., [8], [11], [38], [39] and the references therein. The PDF of a Weibull RV is written as [40]

$$f_W(r) = \frac{k}{\lambda}\left(\frac{r}{\lambda}\right)^{k-1} e^{-(r/\lambda)^k}, \quad r \geq 0 \tag{16}$$

And the PDF of a CG RV with inverse Gamma texture is expressed as [38]

$$f_{CG}(r) = \frac{2r\rho\Gamma(\nu+1)}{(\rho r^2+1)^{\nu+1}\Gamma(\nu)}, \quad r \geq 0 \tag{17}$$

where ν and ρ are shape and scale parameters, respectively.

First, we carry out the fitting comparisons of the proposed model against the Weibull and CG distributions, using four groups of randomly selected data, that is, the 1st range cell of data 005 and 011, the 20th range cell of data 020, and the 35th range cell of data 026. Intuitively, as show in Fig. 6 to Fig. 9, we observe that the fitting to these data using the proposed ARMA-NGARCH-JSU models is better than that using other two distributions, especially for the tail part. It is noted that the model orders used for these simulations are chosen as (1,1,1,0), since according to a large number of simulated results, the estimates of coefficient β_j in conditional variance is less than 10^{-3}, which do not appear to be statistically significant. Moreover, increasing the order of AR and MA terms does not necessarily improve modeling accuracy, since higher order model requires larger amount of training data, which is subject to the radar dwell time and PRF. Also, the parameter estimation will be more time-consuming.

To quantitatively evaluate the fitting accuracy, the Kolmogorov-Smirnov (K-S) statistical distance [41] is

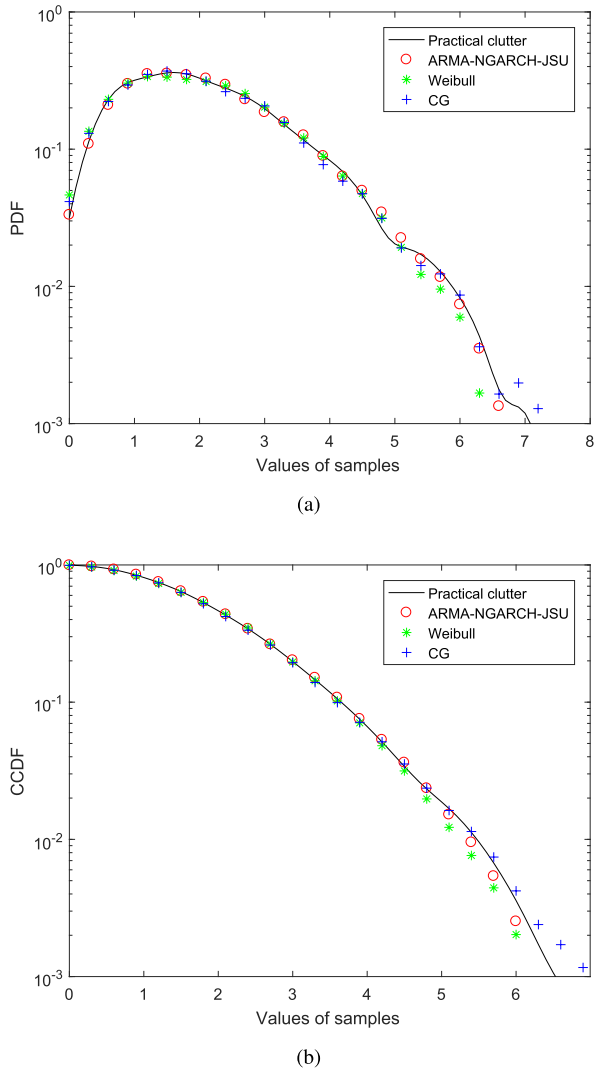

FIGURE 9. Fitted PDFs (a) and CCDFs (b) for the 35th range cell of data 026.

calculated, which is expressed as

$$D_{KS} = \max_{1 \le i \le N} |F(x_i) - F_t(x_i)| \tag{18}$$

where $F(x_i)$ and $F_t(x_i)$ are the empirical and theoretical CDF, respectively, and N is the number of samples. Using the same data as in Fig. 6 to Fig. 9, the statistical results are reported in Table 3. It is seen that the ARMA-NGARCH-JSU process always achieves the minimum value, which indicates the applicability and flexibility of the proposed model. This improvement is common not only for the selected data, but also other available measurements when the same procedures are conducted, including other range cells of the selected data and other data sets.

Moreover, taking range cell 35 of data 026 as a example, Fig. 10 displays the quantile-quantile plot (QQ-plot) [42] of the quantiles of the clutter amplitude versus the quantiles of the synthetic ARMA-NGARCH-JSU samples using the coefficients estimated from the practical clutter measurements.

TABLE 3. Results of K-S statistical distance for various data sets.

Data (Range cell)	ARMA-NGARCH-JSU	Weibull	CG
005 (1)	0.0065	0.0077	0.0093
011 (1)	0.0070	0.0202	0.0100
020 (20)	0.0169	0.0234	0.0182
026 (35)	0.0092	0.0123	0.0104

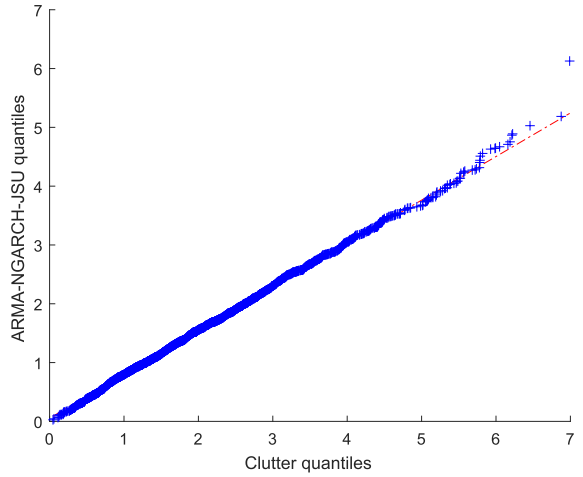

FIGURE 10. QQ-plot of the quantiles of clutter amplitude (range cell 35 of data 026) versus the quantiles of a synthetic ARMA-NGARCH-JSU process.

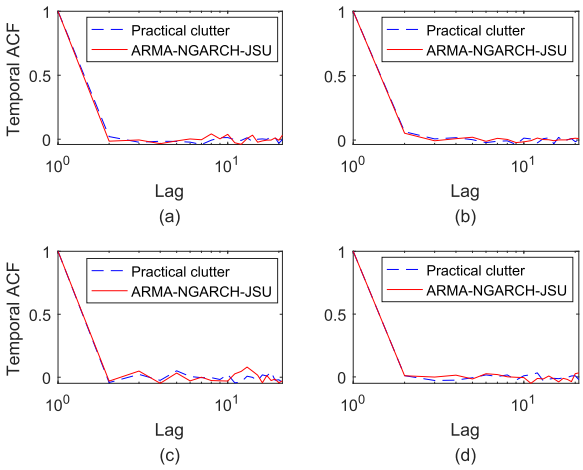

FIGURE 11. Temporal ACF of practical clutter, and of an ARMA-NGARCH-JSU process, using (a) range cell 1 of data 016, (b) range cell 1 of data 020, (c) range cell 1 of data 025, and (d) range cell 35 of data 026.

The purpose of the QQ-plot is to determine whether the samples of two processes come from the same distribution. If the samples do come from the same distribution (same shape), even if one distribution is shifted and re-scaled from the other (different location and scale parameters), the plot will be linear [43]. It is seen that the quantiles of the proposed model is linear in a wide range, which means that the ARMA-NGARCH-JSU model can accurately model the practical clutter amplitude.

Finally, we check the modeling effect of temporal autocorrelation characteristics, using four data sets, i.e., range

cell 1 of data 016, range cell 1 of data 020, range cell 1 of data 025, and range cell 35 of data 026. It is seen from Fig. 11 that the decorrelation time of practical clutter are accurately captured by the proposed model, and the variation tendencies are essentially the same.

VI. CONCLUSION

In this paper, we model the sea clutter as an ARMA time series with GARCH errors. The ARMA terms are used for modeling the temporal correlation, and the GARCH part is used for modeling the heteroskedasticity and volatility clustering. The innovation term is assumed to satisfy the JSU distribution, which is a a monotonic transformation of the normal distribution and is capable of modeling the skewness existing in practical sea clutter measurements. The coefficients of the proposed model are estimated by QMLE method. By systematically analyzing a large number of practical sea clutter data sets, we show that the proposed ARMA-NGARCH-JSU model fits the data better than some commonly used statistic-based distributions, such as the Weibull and CG distributions.

On-going research is focused in the subsequent detection schemes. It is known that the (unconditional) PDF of GARCH-type process do not have explicit expression, and only conditional PDF is available. In traditional generalized likelihood ratio test (GLRT), the corresponding likelihood functions under different hypothesis need to be replaced by their conditional versions. The detection performance also needs further study.

ACKNOWLEDGMENTS

The authors would like to thank the Council for Scientific and Industrial Research of South Africa for publishing the sea clutter data.

REFERENCES

[1] J. Carretero-Moya, J. Gismero-Menoyo, Á. Blanco-del-Campo, and A. Asensio-Lopez, "Statistical analysis of a high-resolution sea-clutter database," *IEEE Trans. Geosci. Remote Sens.*, vol. 48, no. 4, pp. 2024–2037, Apr. 2010.

[2] M. Greco, F. Bordoni, and F. Gini, "X-band sea-clutter nonstationarity: Influence of long waves," *IEEE J. Ocean. Eng.*, vol. 29, no. 2, pp. 269–283, Apr. 2004.

[3] A. Drosopoulos, "Description of the OHGR database," Defence Res. Establishment, Ottawa, ON, USA, Tech. Rep. 94-14, Dec. 1994.

[4] I. Antipov, "Statistical analysis of Northern Australian coastline sea clutter data," Defence Sci. Technol. Org., Edinburgh, SA, Australia, Tech. Rep. DSTO-TR-1236, Nov. 2001.

[5] K. D. Ward, S. Watts, and R. J. Tough, *Sea Clutter: Scattering, The K Distribution and Radar Performance*. Edison, NJ, USA: IET, 2006, vol. 20.

[6] M. Sekine, T. Musha, Y. Tomita, T. Hagisawa, T. Irabu, and E. Kiuchi, "Weibull-Distributed sea clutter," *IEE Proc. F Commun., Radar Signal Process.*, vol. 130, no. 5, p. 476, Aug. 1983.

[7] D. C. Schleher, "Radar detection in Weibull clutter," *IEEE Trans. Aerosp. Electron. Syst.*, vol. AES-12, no. 6, pp. 736–743, Nov. 1976.

[8] R. Ravid and N. Levanon, "Maximum-likelihood CFAR for Weibull background," *IEE Proc. F Radar Signal Process.*, vol. 139, no. 3, pp. 256–264, Jun. 1992.

[9] S. Watts, "Radar detection prediction in K-distributed sea clutter and thermal noise," *IEEE Trans. Aerosp. Electron. Syst.*, vol. 23, no. 1, pp. 40–45, Jan. 1987.

[10] G. V. Trunk and S. F. George, "Detection of targets in non-Gaussian sea clutter," *IEEE Trans. Aerosp. Electron. Syst.*, vol. 6, no. 5, pp. 620–628, Sep. 1970.

[11] K. J. Sangston, F. Gini, and M. S. Greco, "Coherent radar target detection in heavy-tailed compound-Gaussian clutter," *IEEE Trans. Aerosp. Electron. Syst.*, vol. 48, no. 1, pp. 64–77, Jan. 2012.

[12] E. Ollila, D. E. Tyler, V. Koivunen, and H. V. Poor, "Compound-Gaussian clutter modeling with an inverse Gaussian texture distribution," *IEEE Signal Process. Lett.*, vol. 19, no. 12, pp. 876–879, Dec. 2012.

[13] X. Shang and H. Song, "Radar detection based on compound-Gaussian model with inverse gamma texture," *IET Radar Sonar Navigat.*, vol. 5, no. 3, pp. 315–321, Mar. 2011.

[14] J. Hu, W. W. Tung, and J. Gao, "A new way to model nonstationary sea clutter," *IEEE Signal Process. Lett.*, vol. 16, no. 2, pp. 129–132, Feb. 2009.

[15] J. P. Pascual, N. V. Ellenrieder, M. Hurtado, and C. H. Muravchik, "Radar detection algorithm for GARCH clutter model," *Digit. Signal Process.*, vol. 23, no. 4, pp. 1255–1264, 2013.

[16] T. Bollerslev, "Generalized autoregressive conditional heteroskedasticity," *J. Econometrics*, vol. 31, no. 3, pp. 307–327, 1986.

[17] M. Amirmazlaghani, H. Amindavar, and A. Moghaddamjoo, "Speckle suppression in SAR images using the 2-D GARCH model," *IEEE Trans. Image Process.*, vol. 18, no. 2, pp. 250–259, Feb. 2009.

[18] H. Amiri, H. Amindavar, and M. Kamarei, "Underwater noise modeling and direction-finding based on heteroscedastic time series," *Eurasip J. Adv. Signal Process.*, vol. 2007, no. 1, p. 071528, 2006.

[19] J. P. Pascual, N. V. Ellenrieder, M. Hurtado, and C. H. Muravchik, "Adaptive radar detection algorithm based on an autoregressive GARCH-2D clutter model," *IEEE Trans. Signal Process.*, vol. 62, no. 15, pp. 3822–3832, Aug. 2014.

[20] Y. Zhang, J. Shi, Z. Deng, and P. Pan, "Detection in sea clutter based on nonlinear ARCH model," *Digit. Signal Process.*, vol. 50, pp. 162–170, Mar. 2016.

[21] Y. Zhang, Z. Deng, J. Shi, Y. Zhang, and H. Liu, "Sea clutter modeling using an autoregressive generalized nonlinear-asymmetric GARCH model," *Digit. Signal Process.*, vol. 62, pp. 52–64, Mar. 2017.

[22] Y. Zhang, Y. Zhang, Z. Deng, X. P. Zhang, and H. Liu, "Sea surface target detection based on complex ARMA-GARCH processes," *Digit. Signal Process.*, vol. 70, pp. 1–13, Nov. 2017.

[23] D. A. Hsieh, "Modeling heteroscedasticity in daily foreign-exchange rates," *J. Bus. Econ. Stat.*, vol. 7, no. 3, pp. 307–317, 1989.

[24] J. B. Mcdonald and W. K. Newey, "Partially adaptive estimation of regression models via the generalized t distribution," *Econ. Theory*, vol. 4, no. 3, pp. 428–457, 1988.

[25] R. T. Baillie and T. Bollerslev, "The message in daily exchange rates: A conditional-variance tale," *J. Bus. Econ. Stat.*, vol. 7, no. 3, pp. 297–305, 1989.

[26] N. L. Johnson, "Bivariate distributions based on simple translation systems," *Biometrika*, vol. 36, nos. 3–4, pp. 297–304, 1949.

[27] B. E. Hansen, "Autoregressive conditional density estimation," *Int. Econ. Rev.*, vol. 35, no. 3, pp. 705–730, 1994.

[28] P. C. Andreou, "Skewed generalized error distribution of financial assets and option pricing," *Multinat. Finance J.*, vol. 19, no. 4, pp. 223–266, 2000.

[29] J. S. Shang and P. R. Tadikamalla, "Modeling financial series distributions: A versatile data fitting approach," *Int. J. Theor. Appl. Finance*, vol. 7, no. 3, pp. 231–251, 2004.

[30] J.-G. Simonato, "GARCH processes with skewed and leptokurtic innovations: Revisiting the Johnson Su case," *Finance Res. Lett.*, vol. 9, no. 4, pp. 213–219, 2012.

[31] W. Li and A. McLeod, "ARMA modelling with non-Gaussian innovations," *J. Time Ser. Anal.*, vol. 9, no. 2, pp. 155–168, 1988.

[32] P. T. Boggs and J. W. Tolle, "Sequential quadratic programming," *Acta Numer.*, vol. 4, pp. 1–51, 1995.

[33] H. J. De Wind, J. E. Cilliers, and P. L. Herselman, "Dataware: Sea clutter and small boat radar reflectivity databases [best of the web]," *IEEE Signal Process. Mag.*, vol. 27, no. 2, pp. 145–148, Mar. 2010.

[34] P. L. Herselman, C. J. Baker, and H. J. de Wind, "An analysis of X-band calibrated sea clutter and small boat reflectivity at medium-to-low grazing angles," *Int. J. Navigat. Observ.*, vol. 2008, no. 2, 2008, Art. no. 347518.

[35] A. Farina, F. Gini, M. V. Greco, and L. Verrazzani, "High resolution sea clutter data: Statistical analysis of recorded live data," *IEE Proc. Radar, Sonar Navigat.*, vol. 144, no. 3, pp. 121–130, Jun. 1997.

[36] C. M. Jarque and A. K. Bera, "Efficient tests for normality, homoscedasticity and serial independence of regression residuals," *Econ. Lett.*, vol. 6, no. 3, pp. 255–259, 1980.

[37] L. Ljung and G. E. P. Box, "On a measure of lack of fit in time series models," *Biometrika*, vol. 65, no. 2, pp. 297–303, 1978.
[38] X. Shang, H. Song, Y. Wang, C. Hao, and C. Lei, "Adaptive detection of distributed targets in compound-Gaussian clutter with inverse gamma texture," *Digit. Signal Process.*, vol. 22, no. 6, pp. 1024–1030, 2012.
[39] A. Balleri, A. Nehorai, and J. Wang, "Maximum likelihood estimation for compound-Gaussian clutter with inverse gamma texture," *IEEE Trans. Aerosp. Electron. Syst.*, vol. 43, no. 2, pp. 775–779, Apr. 2007.
[40] S. Pillai and A. Papoulis, *Probability, Random Variables and Stochastic Processes*. New York, NY, USA: McGraw-Hill, 2002.
[41] G. W. Corder and D. I. Foreman, *Nonparametric Statistics for Non-Statisticians: A Step-by-Step Approach*. Hoboken, NJ, USA: Wiley, 2009.
[42] M. B. Wilk and R. Gnanadesikan, "Probability plotting methods for the analysis of data," *Biometrika*, vol. 55, no. 1, pp. 1–17, 1968.
[43] S. Mousazadeh and I. Cohen, "AR-GARCH in presence of noise: Parameter estimation and its application to voice activity detection," *IEEE Trans. Audio Speech Language Process.*, vol. 19, no. 4, pp. 916–926, May 2011.

YUNJIAN ZHANG was born in Deyang, Sichuan, China, in 1986. He received the B.E. degree in communication engineering from the Beijing University of Posts and Telecommunications, Beijing, China, in 2008, the M.S. degree in electronics and communication engineering from the University of Electronic Science and Technology of China, Chengdu, China, in 2013, and the Ph.D. degree in communication engineering from the Xiamen University (XMU), Xiamen, China, in 2016. He is currently a Post-Doctoral Research Fellow with the School of Information Science and Engineering, XMU. His research interests include statistical signal processing, parameter estimation, and target detection.

HUI LIU was born in Huangshi, Hubei, China, in 1978. She received the B.S. degree in electronic engineering from Hubei University in 2000, and the M.S. degree and the Ph.D. degree in signal and information processing from Wuhan University, Hubei, China, in 2003 and 2014, respectively. In 2003, she joined the college of Information Science and Technology, Xiamen University, where she is currently an Assistant Professor. Her current research interests include signal detection and parameter estimation, and machine learning.

YANAN HUANG was born in Putian, Fujian, China, in 1994. He received the B.E. degree in communication engineering from Xiamen University (XMU), Xiamen, China, in 2016.He is currently pursuing the master's degree with the School of Informatica Science and Engineering, XMU. His research interests include radar signal processing and parameter estimation.

ZHENMIAO DENG was born in Longyan, Fujian, China, in 1977. He received the B.S. degree in electronic engineering and the Ph.D. degree in signal and information processing from the Nanjing University of Aeronautics and Astronautics (NUAA), Nanjing, China, in 1999 and 2007, respectively. From 2007 to 2009, he was a Post-Doctoral Research Fellow with the College of Automation Engineering, NUAA, involved in the field of signal detection and parameter estimation. In 2010, he joined the College of Information Science and Technology, Xiamen University, where he is currently a Professor. His current research interests include signal detection, parameter estimation, array signal processing, and multirate signal processing.